Disorder-Induced Topological State Transition in Photonic Metamaterials

Changxu Liu, Wenlong Gao, Biao Yang, and Shuang Zhang*
School of Physics and Astronomy, University of Birmingham, Birmingham B15 2TT, United Kingdom
(Received 21 July 2017; published 1 November 2017)

The topological state transition has been widely studied based on the quantized topological band invariant such as the Chern number for the system without intense randomness that may break the band structures. We numerically demonstrate the disorder-induced state transition in the photonic topological systems for the first time. Instead of applying the ill-defined topological band invariant in a disordered system, we utilize an empirical parameter to unambiguously illustrate the state transition of the topological metamaterials. Before the state transition, we observe a robust surface state with well-confined electromagnetic waves propagating unidirectionally, immune to the disorder from permittivity fluctuation up to 60% of the original value. During the transition, a hybrid state composed of a quasiunidirectional surface mode and intensively localized hot spots is established, a result of the competition between the topological protection and Anderson localization.

DOI: 10.1103/PhysRevLett.119.183901

Introduction.—Topological state transitions (TSTs) in electronic systems have been the subject of intensive research in the past decade. The TST was not only predicted by a wide number of theoretical and numerical works [1–9], but also demonstrated experimentally in both two-dimensional and three-dimensional systems [10–14]. The variation of the calculated or measured electronic band structures is the criteria of the TST, which produces a change of the topological invariance such as the Chern number [15]. In spite of a plethora of progress in the realizations of the topological state in photonics [16–26], the research on the TST in optical regime is limited [27–30]. Similarly, the illustration of state transition in photonic systems requires the evaluation of the topological invariance from the photonic band structures or isofrequency surfaces.

The sudden change of the quantized topological invariant across the interface implies the existence of the nontrivial edge or surface states, which are topologically protected against the influence of the disorder [15]. The research on how disorder impacts the topological state in electronic systems has always been the subject of tantalizing interest [31–37]. Not limited to breaking the topological state, recently, it was reported that the disorder could even induce the topological state in trivial systems [38–41]. However, TST triggered by continuously tuning the disorder has remained unexplored yet, probably due to the fact that intense randomness may destroy the spatial translational symmetry, making band structures ill defined in the Brillouin zone. The obstacle in calculating topological invariants makes a definite observation of state transition in a disordered platform challenging.

Despite numerous efforts in the disordered topological states in electronics, quite surprisingly, the photonic counterpart, to the best of our knowledge, is still missing. In this Letter, for the first time, we investigate the influence of the disorder to topological metamaterials in the photonic regime. Instead of utilizing topological invariants, we develop a empirical parameter to elucidate the state transition in the topological system even embedded with prevailing randomness. Based on this newly defined parameter, we succeed in demonstrating a prominent TST numerically as the perturbation in the permittivity gradually increases. Counterintuitively, robust surface states with backscattering immune light transport exist at intense disorder (up to 60% fluctuation to the permittivity) before the TST. During the transition, we demonstrate an intriguing hybrid state composed of a quasiunidirectional propagation surface mode and intensively localized modes nearby. This hybrid state is a result of the competition between topological protection and Anderson localization, and may imply the potential to build a topological random laser with unidirectional emission.

Modeling for the disordered metamaterials.—We select the chiral hyperbolic metamaterial, a photonic Weyl system we developed before as the topological system [17,26]. With respect to some fixed wave vector in the longitudinal (z) direction, it behaves like a Chern insulator with a nonvanishing Chern number defined in the transverse (x-y) dimension [26]. We apply an effective medium approach for the study of the metamaterial, by virtue of its flexibility for disorder introduction, as the fluctuation in electromagnetic parameters. The permittivity ϵ and permeability μ of the uniaxial hyperbolic metamaterial is defined as the following:

$$\bar{\bar{\epsilon}} = \epsilon_0 \bar{\bar{\epsilon}}_r = \epsilon_0 \mathrm{diag}(\epsilon_x, \epsilon_y, \epsilon_z), \mu = \mu_0 \mu_r, \tag{1}$$

with ϵ_0 and μ_0 the permittivity and permeability in vacuum separately. To achieve the topological state in a hyperbolic system, we introduce the chirality γ to break the inverse symmetry, with constitutive relations

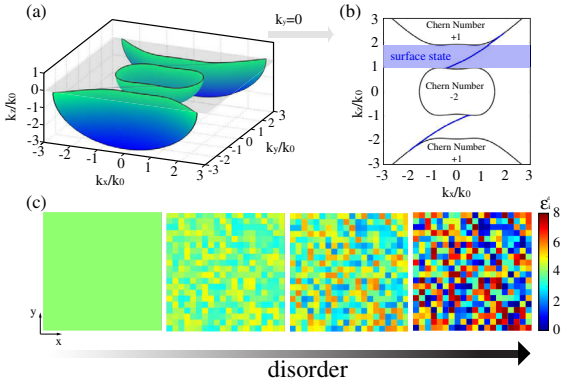

FIG. 1. (a) Equal frequency surfaces of a chiral hyperbolic metamaterial. (b) Cross section of the equal frequency surfaces at $k_y = 0$. The blue solid line corresponds to the surface states. (c) The spatial distribution of ϵ_i^d in the x-y plane for $\sigma_i = 0$, 1, 2, 4, separately.

$$\mathbf{D} = \bar{\bar{\epsilon}}\mathbf{E} - i\gamma\mathbf{H}/c, \mathbf{B} = \mu\mathbf{H} + i\gamma\mathbf{E}/c. \tag{2}$$

Following our previous Letter [17], we choose $\bar{\bar{\epsilon}}_r = \mathrm{diag}(4, 4, -3)$, $\mu_r = 0.5$, and $\gamma = 0.5$. The corresponding equal frequency surfaces are depicted in Figs. 1(a) and 1(b), with calculated Chern number labeled on the equal frequency surfaces separately [17]. The difference between the Chern numbers results in the topologically protected surface states between the wave vector $k_z = \pm 0.91 k_0$ and $k_z = \pm 1.91 k_0$, with $k_0 = 2\pi/\lambda_0$ the wave vector in the free space and k_z the wave vector in the z direction. Owing to the symmetry of the surfaces, we focus on the upper part $k_z > 0$ here.

To embed randomness to our metamaterial-based platform, we introduce the perturbation to the background permittivity $\bar{\bar{\epsilon}}$ as the following:

$$\epsilon_i^d(x, y, z) = \epsilon_i + \sigma_i \delta\epsilon_i(x, y, z), \tag{3}$$

with $i = x$, y, z, and $\delta\epsilon_i$ a spatial random variable with uniform distribution between 0 and 1. And σ_i is a parameter that quantitatively describes the disorder embedded in the system. For each pixel of the fluctuation, we select the size as $\lambda_0/2$, i.e., the wavelength inside the metamaterial. Figure 1(c) plots the spatial distribution of the ϵ_i^d in the x-y plane as the disorder σ_i increases from 0 to 4.

Results.—We investigate the disordered metamaterial with full-wave simulations based on the finite element method in the frequency domain. COMSOL is used to simulate the propagation of surface states at the interface between the topological metamaterial with permittivity fluctuations and the vacuum. Without loss of generality, we analyze the system with continuous translational invariance in the z direction, thereby conserving k_z.

In the regime with dominating randomness [such as the case shown in the very right of Fig. 1(b)], the calculation of the topological band invariant becomes formidably challenging, owing to the nonexistence of the well-defined band structures. Instead, we develop a new empirical parameter $\mathcal{C}_s$ to inspect the TST as the following:

$$\mathcal{C}_s = \frac{\int_{\Pi_s} \mathcal{E}(x, y) dx dy}{\int_{\Pi} \mathcal{E}(x, y) dx dy}, \tag{4}$$

with $\mathcal{E}$ the electromagnetic energy density, Π the whole area of the metamaterial, and Π_s the area with a distant of $\lambda_0/2$ away from the boundary where surface states locate. For a system without randomness, all the electromagnetic energy is confined in the area Π_s because of the topological protection, and $\mathcal{C}_s \simeq 1$. When the perfect protection is diminished by disorder, part of the energy penetrates into the bulk material, leading to the degradation of the surface confinement and the deviation of $\mathcal{C}_s$ from one. The distance $\lambda_0/2$ we choose guarantees the nearly unit value of $\mathcal{C}_s$ without randomness while it demonstrates sharp change at the transition. Therefore, the state transition in topological systems can be feasibly detected by the figure of merit $\mathcal{C}_s$ that represents the quality of the surface localization.

For the first step, we fix the out-of-plane wave vector k_z to $1.5k_0$ that lies in the middle of the values of k_z supporting topological surface states [blue shading area in Fig. 1(b)]. And we consider the general situation that the disorder contributes equally to ϵ_x and ϵ_y, $\sigma_x = \sigma_y = \sigma$. In all simulations, an absorbing layer [as shown in Fig. 2(a)] with the same material properties as our topological metamaterial except for a large imaginary component added to the permittivity has been used to prevent the surface waves from interfering with themselves, allowing the unidirectionality of the boundary modes to be seen clearly.

Figure 2 illustrates the spatial distribution of out-of-plane electrical field E_z and the light intensity I as the increment of the fluctuation σ, demonstrating disorder-induced TST qualitatively. All the E_z are normalized to the maximum value E_m and the intensities I are depicted in logarithm scale to magnify the variation of the confinement of the surface states. Correspondingly, we calculate the $\mathcal{C}_s$ as defined in Eq. (4) for the quantitative investigation of the TST, as shown in Fig. 3.

When $\sigma = 0$, there is no disorder introduced to the system. The electromagnetic energy is well confined with $\mathcal{C}_s \simeq 1$, propagating unidirectionally along the surface, as shown in Figs. 2(a) and 2(f). As the permittivity perturbation increases ($\sigma < 2.5$), quite counterintuitively, no apparent decrement is observed for the value of $\mathcal{C}_s$, implying a robustly protected confinement at the surface between the metamaterial and the vacuum. Accordingly, Figs. 2(b), 2(c) and 2(g), 2(h) illustrate the field or intensity distributions under moderate disorder. In spite of the deformation of the electric field and the nonuniformity of the intensity, the surface states are still well protected. At $\sigma = 2$, the disorder barely leads to 1% of the energy leakage to the bulk,

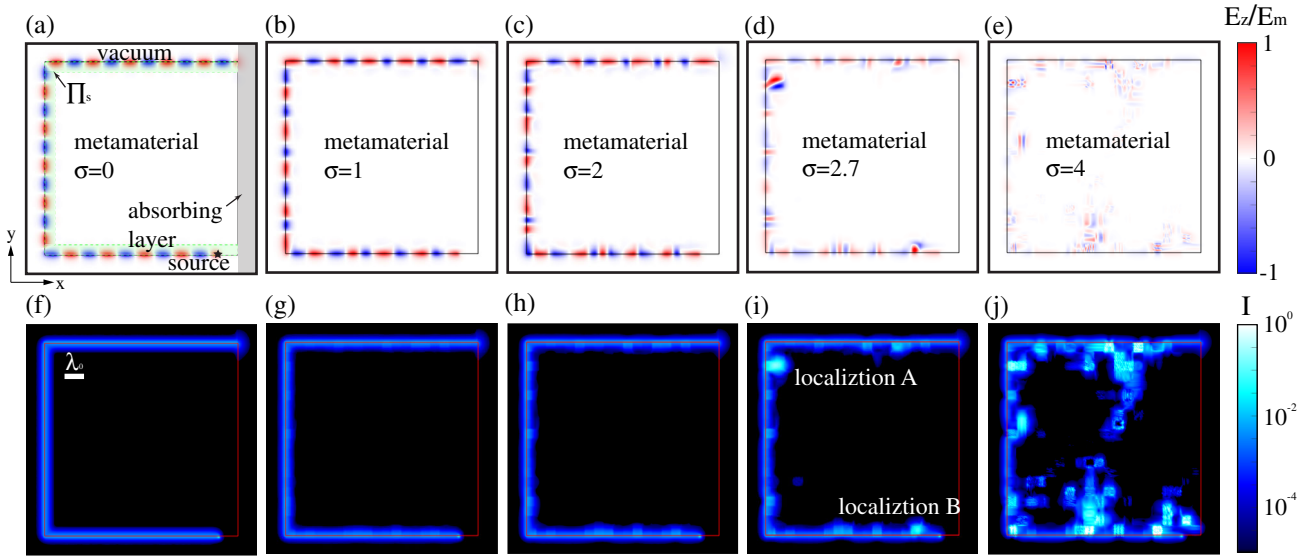

FIG. 2. (a)–(e) Normalized E_z in the disorder-perturbed metamaterial for different values of σ. (f)–(j) The corresponding intensities of the field $I = |\mathbf{E}|^2$ for different values of σ.

demonstrating the robustness of the topological surface states.

Around $\sigma = 2.5$, the value of C_s starts to decrease significantly, providing an unambiguous demonstration of the TST. Figures 2(d) and 2(i) illustrate the electric field E_z and the intensity I at the state transition, separately. Remarkably, as a result of photonic Anderson localization [42–44], we observe that the electromagnetic waves tightly trapped in some region near the surface [such as localization A and B shown in Fig. 2(i)]. Meanwhile, despite the drastically reduced amplitude, the unidirectional propagation at the surface still exists, as shown in Fig. 2(d). At the state transition point, the competition between the topological protection and the Anderson localization produces the hybrid state, including a quasisurface mode and intense localizations, as shown in Fig. 2(i). To investigate the details of this hybrid state, we illustrate the zoomed intensity distribution with Poynting vectors around localization A and B in Fig. 4. Poynting vectors are normalized to clarify the directions of the energy propagation, while the color map of the intensity is switched to linear scale to demonstrate the good quality of the optical confinement that results from Anderson localization. The Poynting vectors form a loop around the localized hot spot, leading to strong confinement of the electromagnetic energy while the Poynting vectors almost keep unidirectional at the surface away from the localization. By virtue of the property of the hyperbolic metamaterials, the direction of the energy propagating is opposite to the direction of the wave propagation [45]. To illuminate that the confinement demonstrated here is due to the Anderson localization instead of the local refractive index difference between

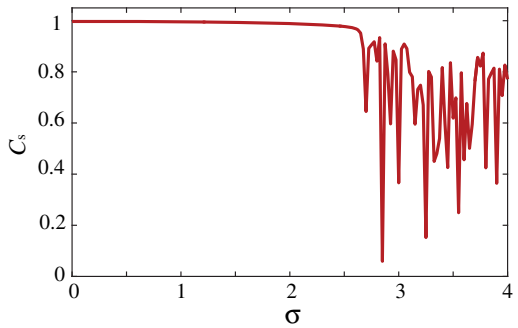

FIG. 3. The topological state transition induced by the disorder in the permittivity at $k_z = 1.5k_0$.

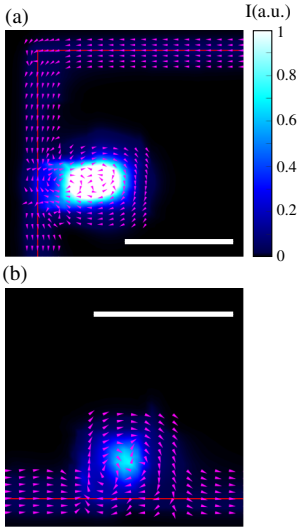

FIG. 4. The hybrid states for (a) localization A and (b) localization B. The magenta arrows are the normalized Poynting vectors. The white scale bar corresponds to the wavelength in vacuum.

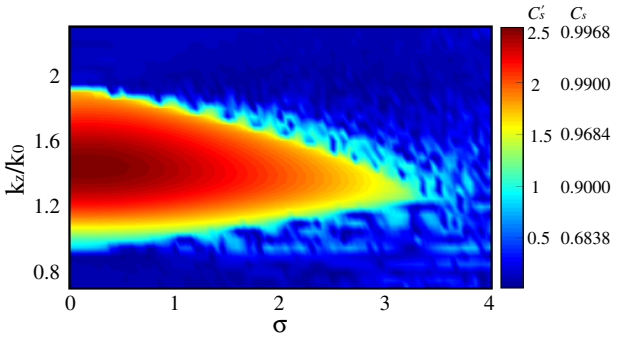

FIG. 5. Disorder-induced topological state transition for different k_z.

fluctuating pixels [as shown in Fig. 1(c)], we inspect the spacial distribution of the refractive index and no prominent index gradient was observed around the localization region. In addition, the localization is not enhanced monotonically with the disorder, excluding the trivial contribution from the local permittivity contrast. More details can be found in the Supplemental Material [46].

As the permittivity perturbation further increases, the hyperbolic properties of the metamaterial are completely destroyed and the surface state shown in Fig. 1(b) is eliminated by the disorder. The electromagnetic waves can penetrate and get trapped inside the bulk, as illustrated in Figs. 2(e) and 2(j). The value of $\mathcal{C}_s$ fluctuates and no surface state can be found. Different random seeds of $\delta\epsilon_i(x, y)$ are implemented and we obtain almost the same results (as shown in the Supplemental Material [46]), exhibiting the generality of the disorder-induced state transition in topological metamaterials.

Instead of using a fixed value of k_z, we next implement the analysis for the disorder-perturbed metamaterials at different k_z. Figure 5 summarizes the result of k_z-dependent TST. To illustrate the value close to 1, we applied a logarithm scale in the color map, $\mathcal{C}_s' = \log_{10}(1 - \mathcal{C}_s)^{-1}$. At $\sigma = 0$, the modes with k_z between $0.91k_0$ and $1.91k_0$ have the value of $\mathcal{C}_s$ close to 1, corresponding to the k_z locating in the blue shaded region in Fig. 1(b). As the embedded randomness inside the system enhances, the surface states with k_z near the equal frequency surface edges are bleached. The surface modes located at the center have the best robustness, immune to stronger permittivity perturbation. Finally, all the topologically protected surface states are annihilated as expected, when the disorder dominates the system.

Discussion.—Although disorder-induced transition has been reported in other fields [47–50], here we demonstrate the topological state transition stimulated by disorder in photonic systems for the first time, to the best of our knowledge. The Chern number as a topological invariant is well defined on the k space when the translation symmetry is imposed on the system. The presence of disorder makes the concept of k space ill defined. Here an empirical $\mathcal{C}_s$ is developed in the disordered system to unambiguously illustrate the state transition of the topological metamaterial. While the $\mathcal{C}_s$ used here is not a well-defined order parameter such as Chern number or $\mathbb{Z}_2$ invariant describing the phase transition in different systems ranging from optical lattices [2], waveguide arrays [28], layer materials [5,6,8,9], and semiconductor heterostructures [3,7,10,13], the sharp transition we numerically demonstrated may stimulate the efforts to seek the counterpart of the Chern number in real space for further analytical explanation [51]. Spatial translation symmetry is believed to be the essence in the realization of a three dimensional Weyl system, because it can prohibit the hybridization between Weyl-node pairs [52]. However, through the numerical study here, we claim that Weyl system is immune to appropriate breaking of translation symmetries, such as the x-y plane here, where the generalized Weyl system is defined in a hybridized parameter space (x, y, k_z).

Not only limited to the interest of fundamental science, our investigation of disorder-induced TST in photonic system is also of practical significance. Our numerical study elucidates the robustness of the topological surface states under disorder, shedding light on the fabrication of topological photonics. To achieve designed property, periodic structures with the feature size comparable with or even smaller than the wavelength is a prerequisite. The numerical results evidence that the functionality does not experience noticeable degradation with moderate degree of disorder, which may relieve the strict tolerance in the fabrication and push topological system to the optical regime. For example, by virtue of the scalability of the Maxwell's equations, the topological system designed for the microwaves [26] may be scaled down to infrared region, in spite of the fabrication imperfection.

Around the topological state transition stage, we discovered the hybrid state with localizated hot spots near the uni-directional surface states, illustrating the potential of interweaving the random laser [53–56] and disordered topological system as a topological random laser. The disorder-induced localization automatically forms an optical cavity with desired confinement. Interestingly, as a result of the topological surface protection, the "cavity" can only be pumped from one direction, as demonstrated from the Poynting vectors in Fig. 4. Accordingly, the emission from the cavity is also forced to propagate along the surface in the same direction for a specific mode within region I. The combination of unparalleled properties of topology and disorder may lead to the realization of a random laser with unidirectional emission.

The work is partially supported by H2020 European Research Council Project No. 648783 (TOPOLOGICAL) and No. 734578 (D-SPA), Leverhulme Trust (Grant No. RPG-2012-674), the Royal Society, and the Wolfson Foundation.

*s.zhang@bham.ac.uk

[1] S. Murakami, New J. Phys. **9**, 356 (2007).
[2] B. Wunsch, F. Guinea, and F. Sols, New J. Phys. **10**, 103027 (2008).
[3] R. M. Lutchyn, J. D. Sau, and S. D. Sarma, Phys. Rev. Lett. **105**, 077001 (2010).
[4] S.-L. Yu, X. C. Xie, and J.-X. Li, Phys. Rev. Lett. **107**, 010401 (2011).
[5] Z. Qiao, W.-K. Tse, H. Jiang, Y. Yao, and Q. Niu, Phys. Rev. Lett. **107**, 256801 (2011).
[6] M. Ezawa, Phys. Rev. Lett. **110**, 026603 (2013).
[7] W. Liu, X. Peng, C. Tang, L. Sun, K. Zhang, and J. Zhong, Phys. Rev. B **84**, 245105 (2011).
[8] Z. Zhu, Y. Cheng, and U. Schwingenschlögl, Phys. Rev. Lett. **108**, 266805 (2012).
[9] Y. Ma, L. Kou, X. Li, Y. Dai, S. C. Smith, and T. Heine, Phys. Rev. B **92**, 085427 (2015).
[10] B. A. Bernevig, T. L. Hughes, and S.-C. Zhang, Science **314**, 1757 (2006).
[11] S.-Y. Xu, Y. Xia, L. Wray, S. Jia, F. Meier, J. Dil, J. Osterwalder, B. Slomski, A. Bansil, H. Lin *et al.*, Science **332**, 560 (2011).
[12] L. Wu, M. Brahlek, R. V. Aguilar, A. V. Stier, C. M. Morris, Y. Lubashevsky, L. S. Bilbro, N. Bansal, S. Oh, and N. P. Armitage, Nat. Phys. **9**, 410 (2013).
[13] J. Zhang, C.-Z. Chang, P. Tang, Z. Zhang, X. Feng, K. Li, L.-l. Wang, X. Chen, C. Liu, W. Duan *et al.*, Science **339**, 1582 (2013).
[14] C. Yan, J. Liu, Y. Zang, J. Wang, Z. Wang, P. Wang, Z.-D. Zhang, L. Wang, X. Ma, S. Ji, K. He, L. Fu, W. Duan, Q.-K. Xue, and X. Chen, Phys. Rev. Lett. **112**, 186801 (2014).
[15] B. A. Bernevig and T. L. Hughes, *Topological Insulators and Topological Superconductors* (Princeton University Press, Princeton, NJ, 2013).
[16] L. Lu, J. D. Joannopoulos, and M. Soljačić, Nat. Photonics **8**, 821 (2014).
[17] W. Gao, M. Lawrence, B. Yang, F. Liu, F. Fang, B. Béri, J. Li, and S. Zhang, Phys. Rev. Lett. **114**, 037402 (2015).
[18] S. Mittal, S. Ganeshan, J. Fan, A. Vaezi, and M. Hafezi, Nat. Photonics **10**, 180 (2016).
[19] M. Xiao, Q. Lin, and S. Fan, Phys. Rev. Lett. **117**, 057401 (2016).
[20] W.-J. Chen, M. Xiao, and C. T. Chan, Nat. Commun. **7** 13038 (2016).
[21] X. Cheng, C. Jouvaud, X. Ni, S. H. Mousavi, A. Z. Genack, and A. B. Khanikaev, Nat. Mater. **15**, 542 (2016).
[22] S. Weimann, M. Kremer, Y. Plotnik, Y. Lumer, S. Nolte, K. G. Makris, M. Segev, M. C. Rechtsman, and A. Szameit, Nat. Mater. **16**, 433 (2017).
[23] A. Slobozhanyuk, S. H. Mousavi, X. Ni, D. Smirnova, Y. S. Kivshar, and A. B. Khanikaev, Nat. Photonics **11**, 130 (2017).
[24] D. Jin, T. Christensen, and M. Soljačić, N. X. Fang, L. Lu, and X. Zhang, Phys. Rev. Lett. **118**, 245301 (2017).
[25] L. Lu, C. Fang, L. Fu, S. G. Johnson, J. D. Joannopoulos, and M. Soljacic, Nat. Phys. **12**, 337 (2016).
[26] B. Yang, Q. Guo, B. Tremain, L. E. Barr, W. Gao, H. Liu, B. Béri, Y. Xiang, D. Fan, A. P. Hibbins, and S. Zhang, Nat. Commun. **8**, 97 (2017).
[27] H. N. Krishnamoorthy, Z. Jacob, E. Narimanov, I. Kretzschmar, and V. M. Menon, Science **336**, 205 (2012).
[28] Y. Ke, X. Qin, F. Mei, H. Zhong, Y. S. Kivshar, and C. Lee, Laser Photonics Rev. **10**, 995 (2016).
[29] A. Blanco-Redondo, I. Andonegui, M. J. Collins, G. Harari, Y. Lumer, M. C. Rechtsman, B. J. Eggleton, and M. Segev, Phys. Rev. Lett. **116**, 163901 (2016).
[30] S. Kruk, A. Slobozhanyuk, D. Denkova, A. Poddubny, I. Kravchenko, A. Miroshnichenko, D. Neshev, and Y. Kivshar, Small **13** 1603190 (2017).
[31] L. Fu, C. L. Kane, and E. J. Mele, Phys. Rev. Lett. **98**, 106803 (2007).
[32] K. Nomura and N. Nagaosa, Phys. Rev. Lett. **106**, 166802 (2011).
[33] G. Schubert, H. Fehske, L. Fritz, and M. Vojta, Phys. Rev. B **85**, 201105 (2012).
[34] K. Kobayashi, T. Ohtsuki, and K.-I. Imura, Phys. Rev. Lett. **110**, 236803 (2013).
[35] J. H. García, L. Covaci, and T. G. Rappoport, Phys. Rev. Lett. **114**, 116602 (2015).
[36] J. H. Bardarson, P. W. Brouwer, and J. E. Moore, Phys. Rev. Lett. **105**, 156803 (2010).
[37] E. Prodan, T. L. Hughes, and B. A. Bernevig, Phys. Rev. Lett. **105**, 115501 (2010).
[38] J. Li, R.-L. Chu, J. K. Jain, and S.-Q. Shen, Phys. Rev. Lett. **102**, 136806 (2009).
[39] C. W. Groth, M. Wimmer, A. R. Akhmerov, J. Tworzydło, and C. W. J. Beenakker, Phys. Rev. Lett. **103**, 196805 (2009).
[40] H.-M. Guo, G. Rosenberg, G. Refael, and M. Franz, Phys. Rev. Lett. **105**, 216601 (2010).
[41] A. Agarwala and V. B. Shenoy, Phys. Rev. Lett. **118**, 236402 (2017).
[42] T. Schwartz, G. Bartal, S. Fishman, and M. Segev, Nature (London) **446**, 52 (2007).
[43] C. Conti and A. Fratalocchi, Nat. Phys. **4**, 794 (2008).
[44] H. H. Sheinfux, Y. Lumer, G. Ankonina, A. Z. Genack, G. Bartal, and M. Segev, Science **356**, 953 (2017).
[45] A. Poddubny, I. Iorsh, P. Belov, and Y. Kivshar, Nat. Photonics **7**, 948 (2013).
[46] See Supplemental Material at http://link.aps.org/supplemental/10.1103/PhysRevLett.119.183901 for the trivial role of confinement from the local index contrast.
[47] M.-C. Cha and H. A. Fertig, Phys. Rev. Lett. **74**, 4867 (1995).
[48] D. W. Brown, P. E. Sokol, and S. N. Ehrlich, Phys. Rev. Lett. **81**, 1019 (1998).
[49] T. Vojta, Phys. Rev. Lett. **90**, 107202 (2003).
[50] C. Liu, A. Di Falco, D. Molinari, Y. Khan, B. S. Ooi, T. F. Krauss, and A. Fratalocchi, Nat. Photonics **7**, 473 (2013).
[51] D. Toniolo, arXiv:1708.05912.
[52] X. Wan, A. M. Turner, A. Vishwanath, and S. Y. Savrasov, Phys. Rev. B **83**, 205101 (2011).
[53] D. S. Wiersma, Nat. Photonics **7**, 188 (2013).
[54] H. Cao, Y. G. Zhao, S. T. Ho, E. W. Seelig, Q. H. Wang, and R. P. H. Chang, Phys. Rev. Lett. **82**, 2278 (1999).
[55] B. H. Hokr, J. N. Bixler, M. T. Cone, J. D. Mason, H. T. Beier, G. D. Noojin, G. I. Petrov, L. A. Golovan, R. J. Thomas, B. A. Rockwell, and V. V. Yakovlev, Nat. Commun. **5**, 4356 (2014).
[56] S. Gottardo, R. Sapienza, P. D. García, A. Blanco, D. S. Wiersma, and C. López, Nat. Photonics **2**, 429 (2008).